The 31th Annual International Conference of Iranian Society of Mechanical Engineers & 9th Conference on Thermal Power Plants
9 to 11 May, 2023, Tehran, Iran.

ISME2023-IC1284

An investigation on the effects of using double-airfoil blades on the torque of a Vertical Axis Wind Turbine by means of numerical simulation

Ahmad Nazari Gazik[1], Sobhan Keikha[2], Kourosh Mojarab Naei[3], AbdolHasib Allahyari[4], Farbod Salehi P.[5], Mohammad Hassan Djavareshkian[6]

[1] B.Sc. student in mechanical engineering, Ferdowsi University of Mashhad, Mashhad; Ahmad_Nazari@mail.um.ac.ir
[2] B.Sc. student in Aerospace engineering, Ferdowsi University of Mashhad, Mashhad; Sobhan.keikha@mail.um.ac.ir
[3] B.Sc. student, Ferdowsi University of Mashhad, Mashhad; kourosh_MojarabNaei@mail.um.ac.ir
[4] B.Sc. student in mechanical engineering, Ferdowsi University of Mashhad, Mashhad; allahyari.1379@mail.um.ac.ir
[5] B.Sc. student in mechanical engineering, Ferdowsi University of Mashhad, Mashhad; Farbod.salehi@um.ac.ir
[6] Professor, Ferdowsi University of Mashhad, Mashhad; Javareshkian@um.ac.ir

Abstract
The main purpose of the upcoming article is to investigate the effects of using a blade with two NACA 0015 airfoils with a geometric ratio of 0.5 on the output power of a vertical-axis wind turbine exposed to wind with a constant speed of 10 m/s at different rotational speeds.

Initially, creating a suitable strategy for the numerical simulation of a straight-blade vertical axis wind turbine using a 2D mesh has been discussed. This 2D simulation was done via Ansys 2021 commercial software and results were verified with experimental results. Appropriate settings have been used to solve the issue of not modeling the airfoil edge vortices in a 2D simulation and minimizing its effects. Although in addition to the errors of a 2D modeling, the Reynolds-averaged Navier-Stokes (RANS) solvers have errors compared to the Direct Numerical Simulation method, however different settings and modeling have been used to extract closest results to experimental data. Additionally, the sliding mesh technique has been utilized, which provides lower computational cost than the dynamic mesh technique. The result of this numerical solution has 90% accuracy relative to simulation using SST K-ω model.

Following, based on the validated results and using similar settings, the effects of using double-airfoils in two different modes have been investigated and the results have been compared with the single airfoil turbine. Ultimately, the power coefficient at variable rotational speeds has been evaluated for single and double-airfoil turbines, which indicates the power coefficient of the turbine has increased by 12% on average.

Keywords
Vertical Axis Wind Turbine, Aerodynamics, Computational Fluid Dynamics, Double-Airfoil Blades, Renewable Energies

Introduction

As reported by the Renewable 2017 Global Status Report, since the beginning of the 21st Century, Wind and Solar energy have been the most dominant used renewable energies [1]. The energy mix produced by REN21, as shown in Fig. 1, indicates that the contribution of renewable energy is around 487 GW, with an increase of 11% since 2015. With a contribution of approximately 4%, wind energy leads all other non-conventional renewable energy sources [1].

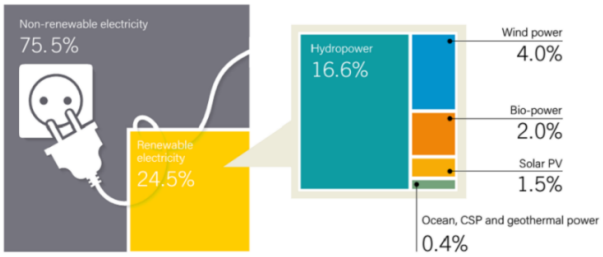

Figure 1. The contribution of different energy production sources in electricity production in the world, End-2016

Horizontal axis wind turbines (HAWT) and vertical axis wind turbines (VAWT) are the two types into which the wind turbines are divided. Due to their massive size and excellent power output capability, HAWTs currently dominate the wind energy market [2]. The benefits of VAWTs, however, have recently received more attention [3]. These benefits include being more suitable for urban environmental applications than the more widely used HAWTs due to a number of important factors, including low maintenance costs, a straightforward blade shape, omnidirectional work capability, and low noise [4].

For VAWT to be commercialized, performance improvement is a crucial requirement. Given its distinctive spinning motion, a VAWT's blade captures the most wind energy on the perimeter facing upwind, and as a result, its power coefficient is typically lower than that of a HAWT [5].

Many researchers have explored ways to improve the performance of the VAWT. Three types of performance-improving techniques exist: modifying the wind turbine layout [6–9], using an additional boost device [10–12], and exploiting of the advantageous aerodynamic interaction between VAWTs [13]. The Savonius wind turbine and the Darrieus wind turbine, both of which are seen in Figure 2, are the two primary varieties of vertical axis wind turbines. [14]

This paper discusses about the second category, the analysis of effect of additional boost device which is a secondary airfoil on the performance of a VAWT.

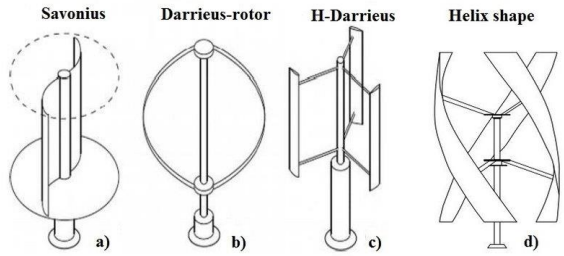

Figure 2. Most widely used configurations of vertical axis wind turbines. A Savonius drag-based wind turbine (figure a) and a straight bladed lift-based Darrieus wind turbine (figure c) can be seen in the figure.

VAWT Model

The turbine used in the experimental tests, which was investigated in the article by Bravo et al. [15], has the following characteristics mentioned in table 1.

Table 1. characteristics of the wind turbine investigated experimentally by Bravo et al.

Parameters	Details
Number of Blades	3
Airfoil	NACA 0015
Blade Height (m)	3
Chord length (m)	0.4
Turbine Radius (m)	1.25
Rotational Speed (rpm)	30-122
Wind Speed ($\frac{m}{s}$)	10
TSR	0.4-1.6

Due to the wide range of parameters involved in the power output produced by a vertical axis wind turbine, Bravo et al. [15] investigated the power output produced by the turbine in varying rotational speed and constant wind speed using appropriate equipment and brake system.

In the first section of the present study, a 2D CFD model has been developed to validate the results of the numerical model with the experimental results. In the second section, using the same 2D CFD model, an investigation of the redesigned rotor of the turbine has been carried out.

The redesign process involves using a smaller secondary NACA 0015 airfoil with chord length of 0.2m near the main NACA 0015 airfoil. In the initial design, the secondary airfoil is placed on top of the main airfoil at a distance of 13cm. In the second design, the secondary airfoil is fixed beneath the main airfoil at a distance equal to 13cm.

Numerical Setup and Boundary Conditions

In this study, the simulations were performed using Ansys 2021. In recent years, SST k-ω turbulence model has been widely used to develop valid simulation of air flow in VAWT studies. After performing the steps corresponding to the numerical simulation, the following calculation domain (Figure 3) has been selected to check the output torque and power coefficient calculated from equation (1).

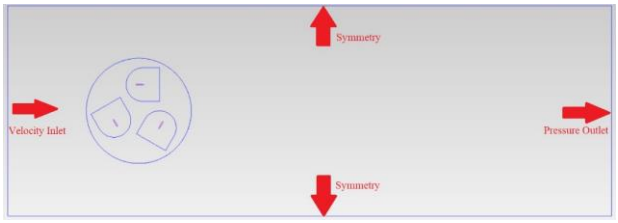

Figure 3. Computational domain and boundary conditions

The center of the rotor is located at a distance of 5 times the distance from the velocity inlet, and the distance from the computation domain outlet is 18 times the radius of the turbine.

Also, the two upper and lower boundaries are 4 times the radius of the turbine rotor from each other. The inlet boundary has the velocity inlet condition and the outlet boundary has the pressure outlet condition. Further, the two upper and lower boundaries were considered as symmetry boundary conditions to eliminate the effect of small domain width. The scope of the solution is selected based on the study by Lanzafame et al. [16].

Meshing

In this study, the sliding mesh technique has been used to simulate the rotation of the turbine and reduce the computational cost for modeling the aerodynamic phenomena around the airfoil. According to the model used for simulation, the boundary layer mesh around the airfoil is created with Y^+ smaller than 1.

Due to the extreme changes in the angle of attack of the airfoil during the rotation of the rotor, in some angles of attack many vortices are created in the region near the airfoil surface. Therefore, in order to better model the flow, it is necessary to use a properly structured mesh around the airfoil. Moreover, due to the better modeling of wake and turbulence by structured mesh compared to unstructured mesh, in the stator part of the solution domain, the structured mesh has been used.

Another major point in the sliding mesh technique is the uniformity of the size of the cells on both sides of the interface boundaries, which is included in the meshing.

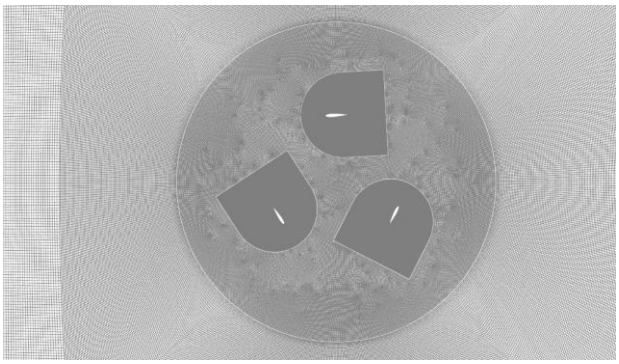

Figure 4. Mesh grid of the solution domain for rotor A

Mesh Grid Independency

To ensure that CFD results do not depend on the mesh density, four meshes were assessed numerically, comprising between 152,000 and 637,000 cells. The C_p

values were extracted at ω=12.8 radians per second. Table 2 summarizes the C_p values obtained with all meshes considered for the 2D VAWT model with NACA0015 airfoils.

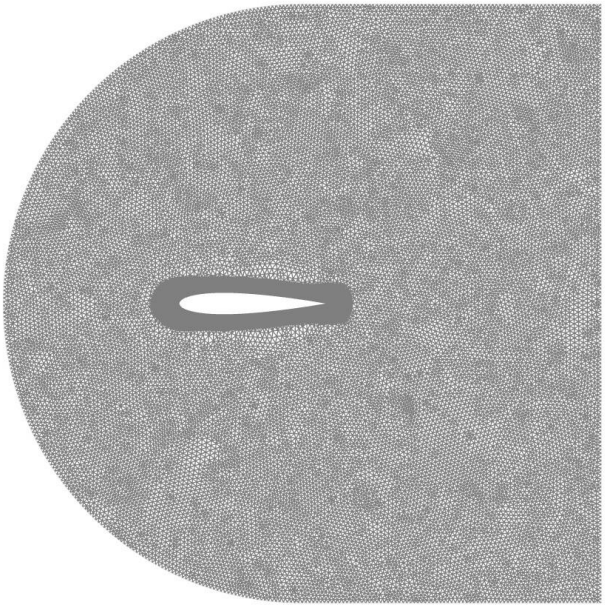

Figure 5. grid generation surrounding the airfoil

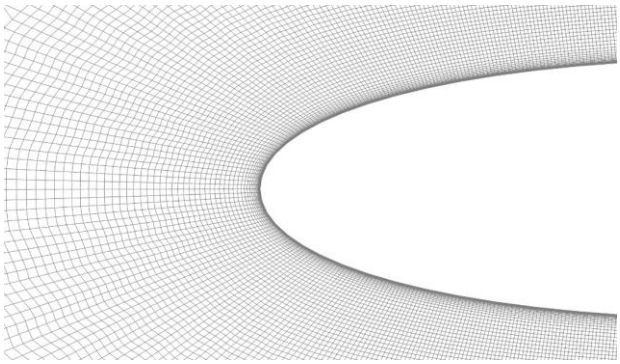

Figure 6. Airfoil leading edge grid generation

Table 2. Results of mesh grid independency

Total Number of cells	Airfoil's regions	Rotor region	Stator region	C_p
152683	91235	30063	31385	0.1768
312543	196490	64859	51194	0.1893
484505	321353	91654	71498	0.1907
637752	398426	106542	132784	0.1913

As it is clear in table 2, there is only 0.3% difference between the results obtained from 484505 cells and 632752 cells. Consequently, to prevent unnecessary computational costs, the mesh with 484505 cells has been selected for the numerical study.

Numerical Simulation Model and Applied settings

Numerical simulation of a 3D experiment using a 2D grid has an unwanted error due to the lack of modeling of the vortices created at the upper and lower edges of each blade. In this simulation, through examining different solvers as well as different discretization methods such as PISO and Coupled discretization methods, the best simulation results were obtained using the SST K-ω model and the PISO discretization method. In the PISO discretization method, the relaxation factors values are adjusted according to the rotational speed of the rotor.

Lanzafame et al.[16] have proposed a time step of 0.0005 seconds for the simulation of the desired wind turbine, thus the flow solution in this research is also based on this time step**.**

Results and Validation

Due to the instability of the solution, an appropriate criterion should be used to detect convergence in solution. To achieve this goal, the solution is considered converged at each time step when the residual values reach 0.001. In addition, the inlet and outlet mass flow rates should be equal in the solution domain. Another parameter is the lift coefficient produced by each blade in each revolution of the turbine, which must be periodical. The most important convergence factor is the periodization of the total torque produced by the turbine in each revolution, which is the best criterion for checking the convergence of the unsteady solution for a wind turbine.

After ensuring that all the convergence conditions of the solution are satisfied, by obtaining the value of the total torque of the turbine in one revolution, the power coefficient for a vertical-axis wind turbine would be calculated using the following equation:

$$C_p = \frac{T\omega}{\frac{1}{2}\rho V^3 A} \quad (1)$$

In the diagram of Figure 7, the experimental test results are compared with the simulation results. In this diagram, the horizontal axis represents the ratio of the rotational speed of the blade tip relative to the wind speed, which can be calculated using the equation (2). Also, the horizontal axis represents the production power factor of the turbine.

$$TSR = \frac{r\omega}{V} \quad (2)$$

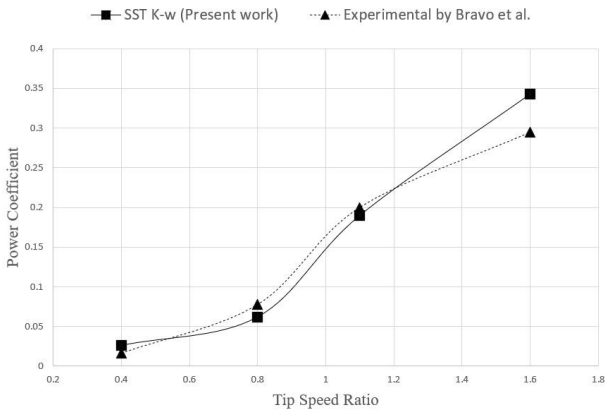

Figure 7. Comparison of the results of numerical simulation and experimental test

As illustrated in the diagram of Figure 7, the results of the numerical simulation with an average error of 10% are consistent with the experimental results and the accuracy

of this simulation can be confirmed. It should be noted that the difference between obtained results and experimental data is increased in rotational speeds higher than 14 radians per second, which is due to the change in the behavior of the vortices on the two edges of the airfoil, which should be solved using the 3D computing mesh and different settings in the mentioned speed rate for more accurate simulation.

The important point is that this simulation has very good accuracy in 80% of the operating range of the turbine.

Results of Design Improvement and Discussion

In this section of the study, the results of using a double-airfoil rotor have been investigated. for this purpose, a secondary NACA0015 airfoil with 0.2 m chord length has been attached to the main airfoil at a distance of 13 cm.

The first design includes the main airfoil and a secondary airfoil on top of the main airfoil (rotor B), while the second design includes the main airfoil and a secondary airfoil at the bottom of the main airfoil (rotor C). Figure 8 illustrates the design of both rotor B and rotor C.

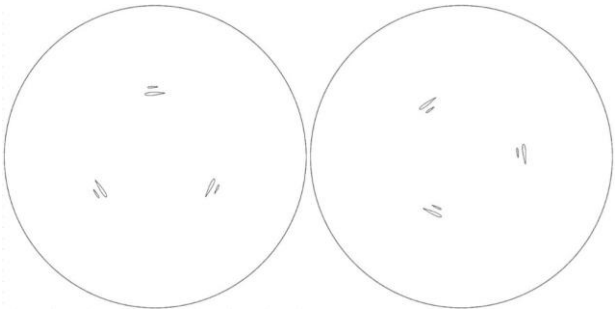

Figure 8. The design of rotor B (left) and rotor C (right).

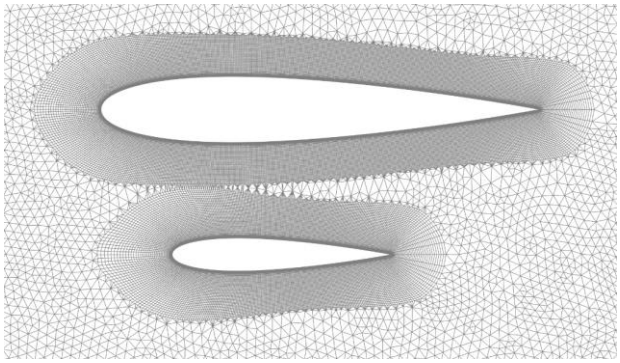

Figure 9. Blade setup and mesh grid around double-airfoil blade for rotor C.

Both rotor B and C have the same mesh grid around the double-airfoil blades, the only difference is in the position of the secondary airfoil which does not affect the number of cells and grid size due to using mesh mirror technique. By applying the same simulation model and criteria as rotor A to rotor B and rotor C, the following results shown in figure 10-12 were obtained.

As it has been shown in figure 10, the decrease in air's kinetic energy and creation of the wake on the right side of the turbine due to transformation of the kinetic energy of air to kinetic energy of the turbine is obvious. Also, extreme stall phenomena and large-scale vortices around the blades of rotor B has been shown in figure 11. The stall phenomena cause significant decrease in the amount of produced lift by the blades. Also, these vortices could cause huge damages to the turbine by increasing the fatigue stress on the blades.

Based on the results obtained from the simulation using the validated model, it has been deemed that although using double-airfoil NACA0015 blades does not affect the starting torque of the wind turbine, but the amount of output power considerably differs between rotor A and two other rotors in higher Tip Speed Ratios.

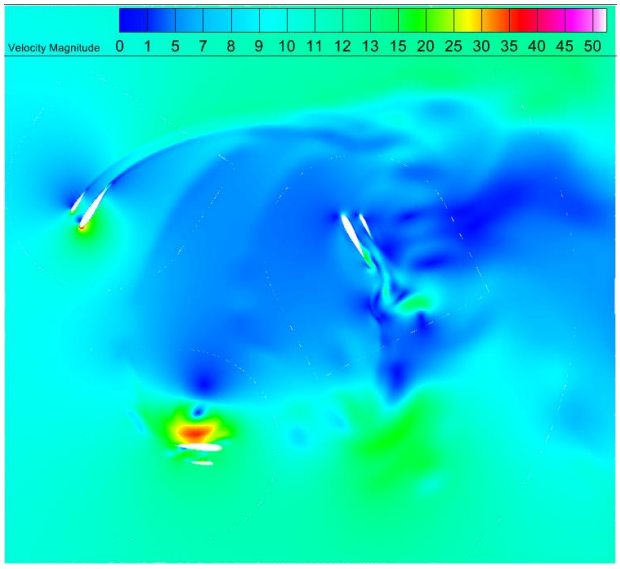

Figure 10. Velocity contour for rotor B at TSR=1.6

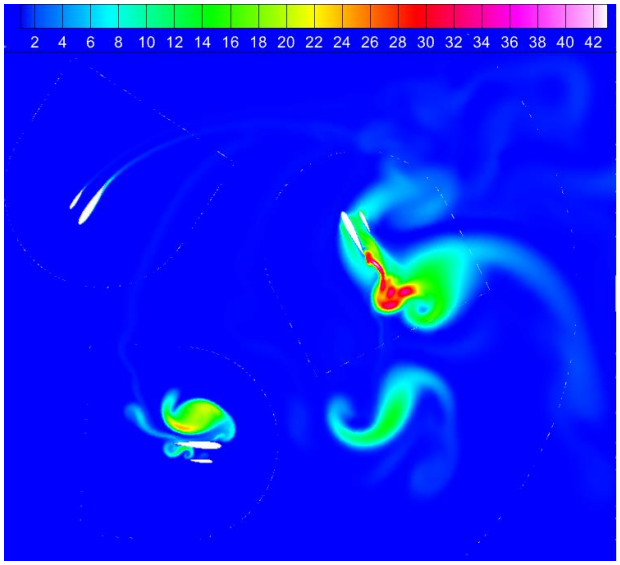

Figure 11. Turbulent Kinetic Energy contour for rotor B at TSR=1.6

At TSR=0.8, although there is no significant difference between rotor A and B, but rotor C has been experienced 60% increase in C_p, which is a significant improvement in the efficiency of the turbine.

At TSR=1.1, rotor A has the highest C_p while rotor C has 46% decrease in C_p. Finally, at higher TSRs, both rotor B and rotor C are able to produce the same amount of power which leads to 20% more power generation than rotor A at TSR=1.6.

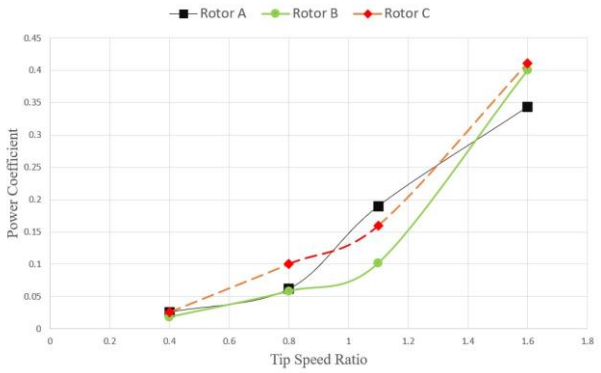

Figure 12. Power coefficient comparison for rotor A, B and C

Conclusions

In this study, a newly designed double-airfoil rotor was investigated numerically using Ansys Fluent. This double-airfoil rotor has been designed using two NACA0015 airfoils. In comparison with the experimental investigation by Bravo [15], the numerical model was deemed capable of predicting the performance of the wind turbine. Although there has been no change in the starting torque of the turbine, the results indicate that the average performance of the turbine is increased by 12% for the double-airfoil rotor with the secondary airfoil beneath the main airfoil. This increase in performance can be considered a significant improvement in the efficiency of an energy extraction process.

Nomenclatures

A Swept Area
C_p Power Coefficient
T Output Torque
V Wind Speed
ρ Air Density
ω Angular Velocity

References

[1] REN21. 2017. "Renewable 2017, Global Status Report". Paris: REN21 Secretariat.

[2] M. N. Kaya, F. Kose, D. Ingham, L. Ma, M. Pourkashanian, 2018. "Aerodynamic performance of a horizontal axis wind turbine with forward and backward swept blades". *Journal of Wind Engineering & Industrial Aerodynamics.*

[3] J. M. Edwards, L. Angelo Danao, R. J. Howell, 2012. "Novel experimental power curve determination and computational methods for the performance analysis of vertical axis wind turbines".

[4] PhD thesis, K. M. Almohammadi, 2014 "Optimization of a CFD Based Design of a Straight Blade Vertical Axis Wind Turbine (SB-VAWT)", The University of Leeds, PhD

[5] J. Liu, H. Lin, J. Zhang, 2019. "Review on the technical perspectives and commercial viability of vertical axis wind turbines". *Ocean Eng.*, 182:608–26. URL https://doi.org/10.1016/j.oceaneng.2019.04.086.

[6] S. Laín, M. Taborda, O. López, 2018. "Numerical study of the effect of winglets on the performance of a straight blade Darrieus water turbine., *Energies*, 11:297. URL https://doi.org/10.3390/en11020297.

[7] M. Elkhoury, T. Kiwata, E. Aoun, 2015 "Experimental and numerical investigation of a three dimensional vertical-axis wind turbine with variable-pitch". *Journal of Wind Engineering and Industrial Aerodynamics*, 139:111–23. URL https://doi.org/10.1016/j.jweia.2015.01.004.

[8] M. Zamani, S. Nazari, S. A. Moshizi, M. J. Maghrebi, 2016. "Three-dimensional simulation of J-shaped Darrieus vertical axis wind turbine". *Energy*, 116:1243–55. URL https://doi.org/10.1016/j.energy.2016.10.031.

[9] N. Ma, H. Lei, Z. Han, D. Zhou, Y. Bao, K. Zhang, et al, 2018. "Airfoil optimization to improve power performance of a high-solidity vertical axis wind turbine at a moderate tip speed ratio". *Energy* 150:236–52. URL https://doi.org/10.1016/j.energy.2018.02.115.

[10] M. Takao, H. Kuma, T. Maeda, Y. Kamada, M. Oki, A. Minoda, 2009. "A straight-bladed vertical axis wind turbine with a directed guide vane row – effect of guide vane geometry on the performance". *Journal of Thermal Science*, 18:54–7. URL https://doi.org/10.1007/s11630-009-0054-0.

[11] D. Kim, M. Gharib, 2014. "Unsteady loading of a vertical-axis turbine in the interaction with an upstream deflector". *Exp Fluids* 55:1658. URL https://doi.org/10.1007/s00348-013-1658-4.

[12] I. Hashem, M. H. Mohamed, 2018. "Aerodynamic performance enhancements of H-rotor Darrieus wind turbine". *Energy*142:531–45. URL https://doi.org/10.1016/j.energy.2017.10.036

[13] J. O. Dabiri, 2011. "Potential order-of-magnitude enhancement of wind farm power density via counter rotating vertical-axis wind turbine arrays". *Rev Sci Instrum*; 77:3A–303A. URL https://doi.org/10.1063/1.3608170

[14] Francesco Castellani, Davide Astolfi, Mauro Peppoloni, 2019. "Experimental Vibration Analysis of a Small Scale Vertical Wind Energy System for Residential Use". machines, 5(7), May, pp. 35–54. URL https://doi.org/10.3390/machines7020035

[15] Bravo R., Tullis S., Ziada S., "Performance Testing of a Small Vertical-Axis Wind Turbine"., Mechanical Engineering Department, McMaster University

[16] Rosario Lanzafame, Stefano Mauro, Michele Messina, 2014. "2D CFD Modeling of H-Darrieus Wind Turbines Using a Transition Turbulence Model". *Energy Procedia*, Vol. 45, 2014, pp. 131-140. URL https://doi.org/10.1016/j.egypro.2014.01.015